A Hot-Cracking Mitigation Technique for Welding High-Strength Aluminum Alloy

The mechanical strain associated with hot cracking is significantly reduced with the introduction of a heat sink trailing a gas tungsten arc welding torch

BY Y. P. YANG, P. DONG, J. ZHANG AND X. TIAN

ABSTRACT. A hot-cracking mitigation technique for gas tungsten arc welding (GTAW) of high-strength aluminum alloy 2024 is presented. The proposed welding technique incorporates a trailing heat sink (an intense cooling source) with respect to the welding torch. The development of the mitigation technique was based on both detailed welding process simulation using advanced finite element techniques and systematic laboratory experiments.

The finite element methods were used to investigate the detailed thermo mechanical behavior of the weld metal that undergoes the brittle temperature range (BTR) during welding. As expected, a tensile deformation zone within the material BTR region was identified behind the weld pool under conventional GTA welding process conditions for the aluminum alloy studied. To mitigate hot cracking, the tensile zone behind the weld pool must be eliminated or reduced to a satisfactory level if the weld metal hot ductility cannot be further improved. With detailed computational modeling, it was found that by the introduction of a trailing heat sink at some distance behind the welding arc, the tensile strain rate with respect to temperature in the zone encompassing the BTR region can be significantly reduced. A series of parametric studies were also conducted to derive optimal process parameters for the trailing heat sink. The experimental results confirmed the effectiveness of the trailing heat sink technique. With a proper implementation of the trailing heat sink method, hot cracking can be completely eliminated in welding aluminum alloy 2024 (AA 2024).

Introduction

Hot cracking has been a subject of intensive studies over the last few decades. Hot cracking occurs during the solidification process due to a combination of metallurgical behavior on cooling and the surrounding thermomechanical conditions. In general, two basic approaches are usually taken: 1) improving the weld and heat-affected zone (HAZ) material ductility and 2) improving the thermomechanical conditions during welding. Historically, the majority of the research work has been focused on the former, *i.e.,* improving the weld and HAZ material ductility.

To reduce the weld material temperature range BTR and to increase its ductility, one documented method is to introduce alloy elements, such as Ti, Zr, V and B in the aluminum alloy electrode. In doing so, the grain structure of the weld metal can be refined, resulting in an improved ductility and resistance to hot cracking (Ref. 1). A variation of this approach is to control the solidification microstructure of the weld metal by using special solidification techniques. For instance, magnetic arc oscillation and electromagnetic stirring have been used to refine weld microstructure and to change solidification orientation (Refs. 2–6). The alternating columnar grains resulting from transverse arc oscillations at a low frequency can be effective in reducing solidification cracking.

However, it has been realized that for some aluminum alloys, such as 2024, the aforementioned techniques may not offer satisfactory results, especially for eliminating liquation cracking. Consequently, thermomechanical-based techniques have received an increasing attention over the recent years. Zacharia (Ref. 7) studied the relationship between the dynamic stress distribution and the observed cracking behavior in a Sigmajig test specimen, particularly near the trailing edge of the weld pool. Feng (Ref. 8) analyzed thermal and mechanical conditions associated with weld metal solidification cracking. As a better understanding of the thermomechanical conditions associated with a hot crack was established, Karlsson (Ref. 9) proposed a local heating approach based on the characteristics of welding-induced stress distribution in a large plate. It was postulated that the local heating of the base metal on

KEY WORDS

Weld Hot Cracking
Aluminum Alloy 2024
High-Strength Aluminum
Trailing Heat Sink
Welding Process Model
Finite Element Modeling
Gas Tungsten Arc Welding
GTAW

Y. P. YANG, P. DONG and J. ZHANG are with the Center for Welded Structures Research, Battelle, Columbus, Ohio. X. TIAN is with Harbin Institute of Technology, Harbin, P.R. China.

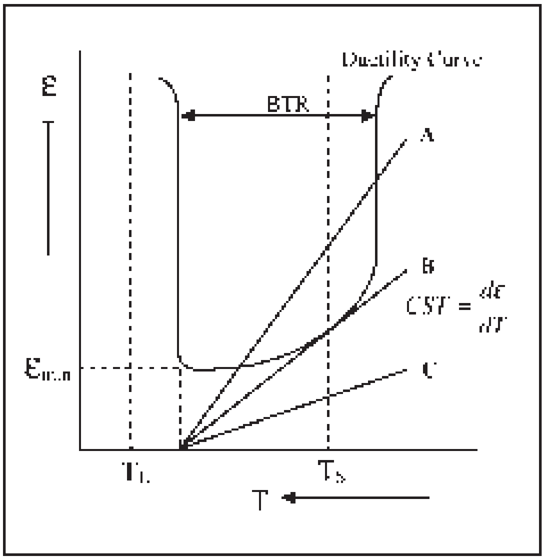

Fig. 1— Thermomechanical conditions associated with hot cracking (Ref. 15).

each side of the weld could produce additional thermal stresses to neutralize tensile stresses in the weld zone. The local heating techniques were also used by Sekiguchi and Mayake (Refs. 10, 11) to overcome end-cracking problems in welding high-strength steel. The end cracks were successfully prevented by preheating the panel to 120°C (248°F), maintaining at a specified inter-pass temperature of 200°C (392°F), and postweld heating of 700°C (1292°F) with a local heating torch. Hernandez and North (Refs. 12, 13) used a pair of oxyacetylene heating torches to heat the base metal on either side to prevent solidification cracking of H30 aluminum alloy sheets.

The mechanisms associated with the local heating methods in preventing hot cracking can be attributed to the fact the transverse and longitudinal strain fields were altered by the use of local heating. For instance, the results obtained by Wu (Ref. 14) indicated the tensile strain rate within the brittle temperature range in the weld zone was reduced with local heating. However, the resulting large HAZ and coarser grain microstructure as a result of local heating have been of concern over its applicability in practice. It was also worth noting local mechanical rolling could also be used to improve the thermomechanical conditions in welding of some simple specimens, as recently illustrated by Liu and Tian (Ref. 15).

In the following, detailed finite element results were presented to characterize the detailed evolution of instantaneous stress and strain behavior associated with hot cracking. A novel welding technique with a trailing heat sink is then proposed to mitigate hot cracking during welding of high-strength aluminum alloys. Parametric studies were conducted to investigate optimal

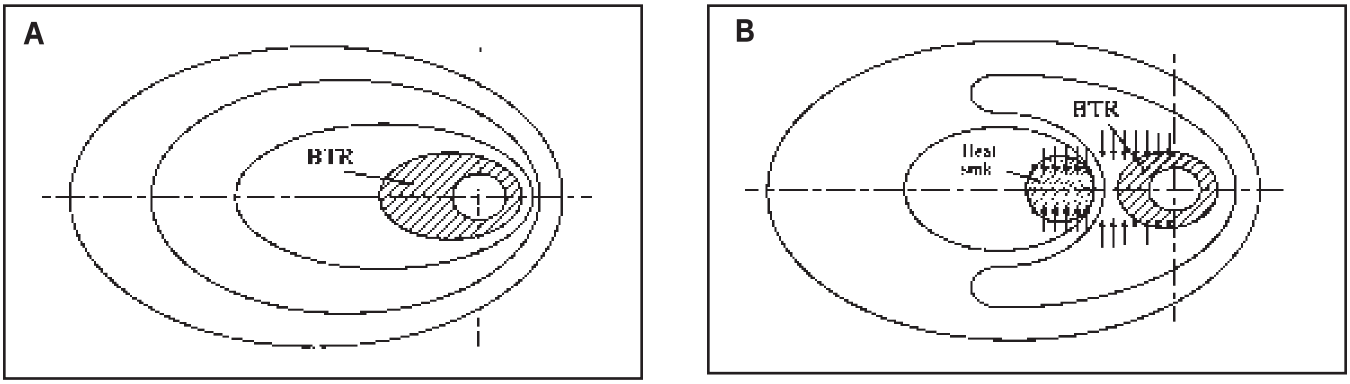

Fig. 2 — Illustration of the effects of a trailing heat sink on isotherms. A — Conventional welding; B — welding with a trailing heat sink.

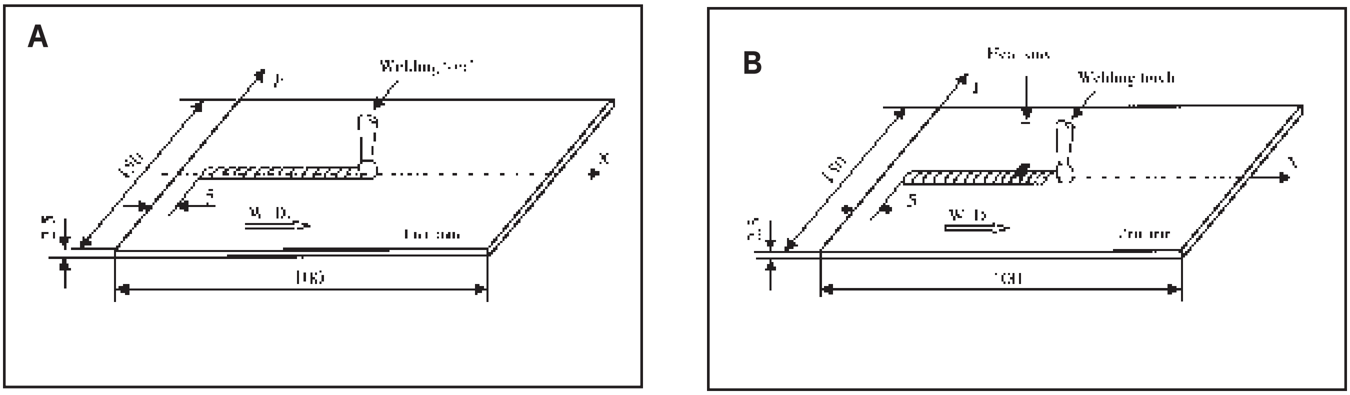

Fig. 3 — Welding conditions and specimen configuration. A — Conventional GTA welding; B — welding with a trailing heat sink.

parameters for the trailing sink. Experimental studies were also carried out to validate the proposed welding technique on high-strength aluminum alloy 2024 panel specimens.

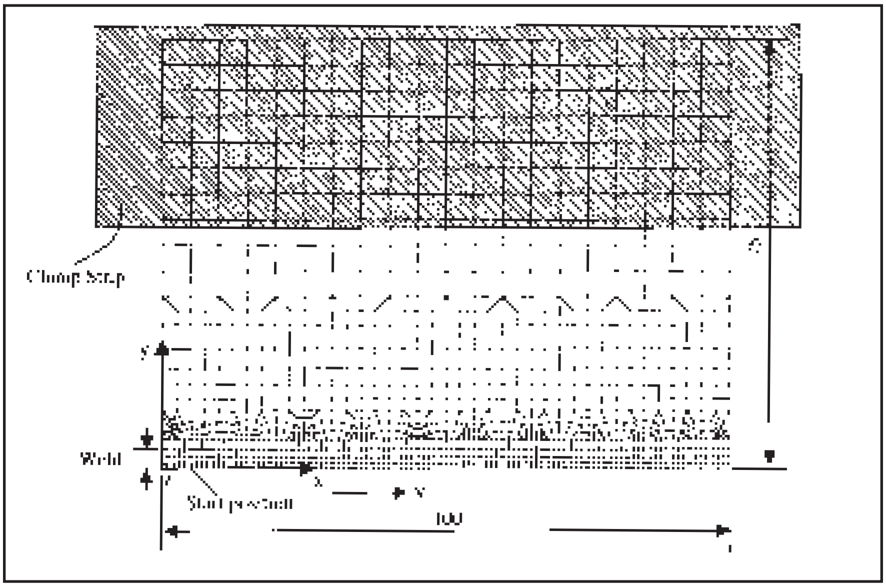

Fig. 4 — Finite element model.

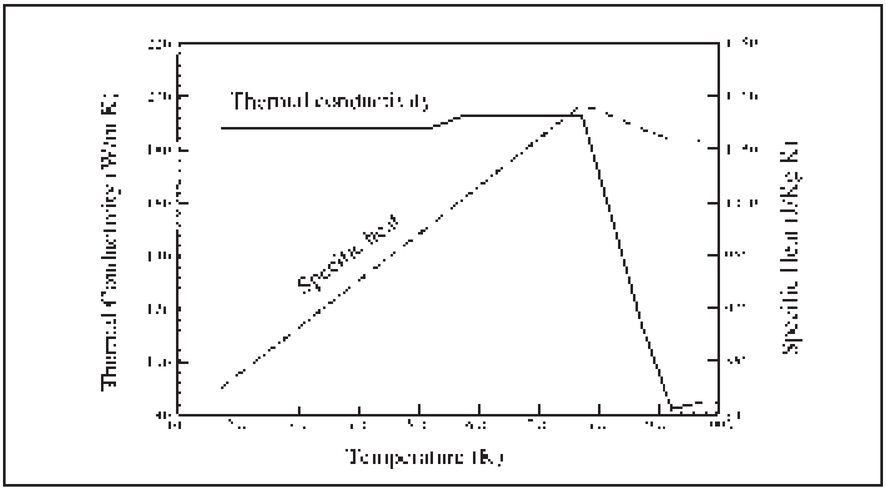

Fig. 5 — Temperature dependence of thermal physical properties for aluminum alloy 2024.

Analysis Procedures

Thermomechanical Conditions for Hot Cracking

The necessary condition for hot cracking is the presence of tensile strains in the region that undergoes the brittle temperature range. Note in this study, mechanical strains were used as a measure of the driving force for hot cracking instead of stresses since at the BTR region the transient stress level is usually low due to significantly reduced material yield strength at high temperature. As depicted in Fig. 1 (Ref. 15), if the tensile strain rate (with respect to temperature) exerting on the BTR region becomes smaller than "the critical strain rate for temperature drop (CST), as depicted by the tangent line (Curve B) to the ductility curve, or

$$\frac{d\varepsilon}{dT} < CST \tag{1}$$

or in theory, hot cracking can be avoided, as depicted by line C. Decomposing $d\varepsilon/dT$, one obtains the following:

$$\frac{d\varepsilon}{dT} = \frac{\partial\varepsilon / \partial t}{\partial T / \partial t} \tag{2}$$

The first term $\partial\varepsilon/\partial t$ in Equation 2 becomes the standard expression of strain rate determined by the thermomechanical response during welding. The second term $\partial T/\partial t$ represents cooling rate typically controlled by the heat flow characteristics of the workpiece under consideration. For a given material, both the strain rate and the cooling rate can be altered by either modifying welding parameters or introducing local heating/cooling mechanisms, or applying mechanical means. For instance, by introducing a trailing heat sink (Fig. 2), an auxiliary compression zone can be generated within the trailing BTR region between the heating source and the heat sink. The effectiveness of the additional compressive strains on the strain rate (with respect to temperature) should be obvious. Assuming a simple additive relationship between welding-induced strain (ε_W) and the strain (ε_c) generated by the heat sink source, the total mechanical strain at any moment in time becomes,

$$\varepsilon = \varepsilon_W - \varepsilon_c \tag{3}$$

and Equation 1 takes the form of

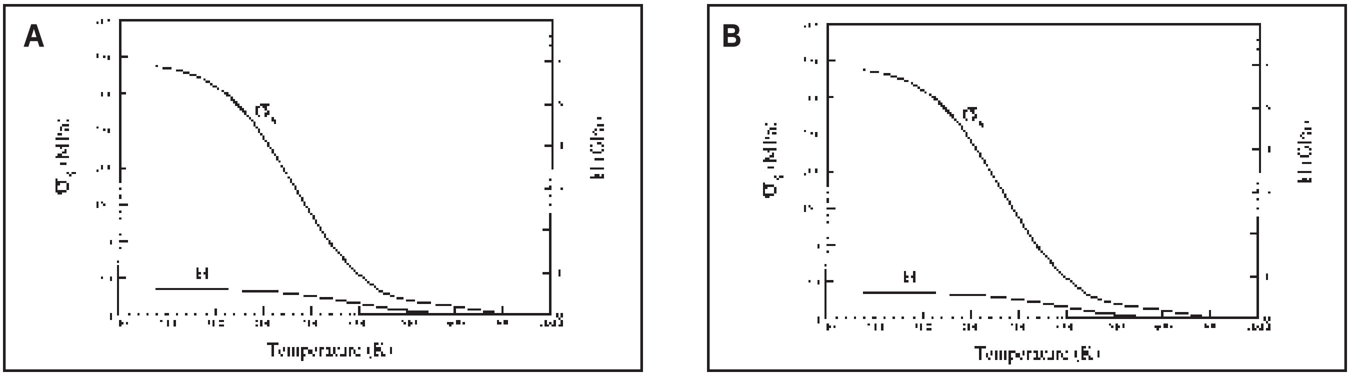

Fig. 6 — Temperature dependence of mechanical properties for AA 2024. A — Elastic modulus E*, thermal expansion α and Poisson's ratio ν; B — Yield stress σ_s and hardening modulus* H.

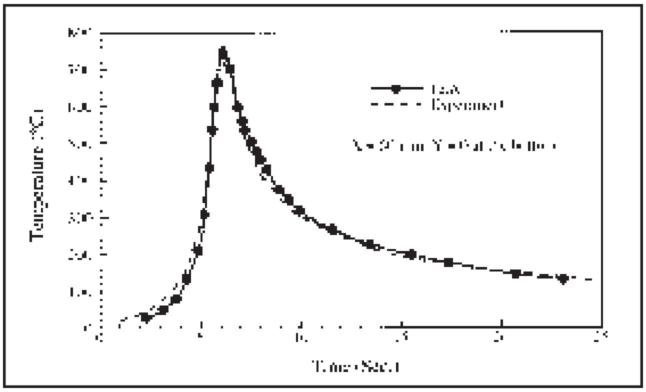

Fig. 7 — Comparison between FE *and experimental results — conventional welding.*

$$\frac{d\varepsilon_w}{dT} - \frac{d\varepsilon_c}{dT} < CST \qquad (4)$$

As a result, hot cracking can be prevented if the reduction of the strain rate with respect to temperature is sufficient within the BTR region. Note the actual reduction of the strain rate (with respect to temperature) is dictated by the complex interactions between the instantaneous strain rate ($\partial\varepsilon/\partial t$) and cooling rate ($\partial T/\partial t$) during welding, as indicated in Equation 2. In the following, advanced finite element procedures were used to quantify and optimize the effects of the trailing heat sink method on the dynamic thermomechanical interactions during welding.

Finite Element Model

As shown in Fig. 3, two types of welding conditions were analyzed. Full penetration bead-on-plate welds were made in the test specimens of aluminum alloy 2024 with a length of 100 mm, width of 150 mm and thickness of 2.5 mm with both conventional GTA welding process (Fig. 3A) and the proposed trailing heat sink technique — Fig. 3B. Both sides of the test specimens parallel to the weld line were clamped tightly by a hydraulic keyboard jig to ensure uniformity of pressure in order to simulate severe restraint conditions in production situations, under which hot cracking was typically observed with the conventional GTA process.

The commercial finite element package *ABAQUS* (Ref. 16) was used in this investigation. As discussed in Refs. 17 and 18, almost all commercial finite element codes are not suited for analyzing the detailed thermomechanical behavior associated with welding. Additional capabilities must be added in the form of user-developed subroutines. In the present study, a unified constitutive law (Ref. 27) was adopted in the form of user-material routine interfaced with *ABAQUS* to simulate the detailed melting and subsequent "annealing" effects. A three-dimensional (3-D) shell element model as shown in Fig. 4 was adopted from an early study (Ref. 17) where its application for modeling multipass welds was presented. With the shell element model, the surface convection heat loss from the top and bottom surfaces of the coupon sheet and the out-of-plane (in z-direction) deformation mode were considered. The through-thickness temperature and deformation gradients were resolved by using five integration points along shell thickness directions based on an early study (Ref. 17). Symmetry conditions were assumed with respect to the centerline of the weld. Fixed displacement boundary conditions (both in-plane and out-of-plane) were imposed at clamp positions (Fig. 4) to simulate the clamping conditions during welding.

Moving Arc and Trailing Heat Sink

A moving heat source model was used as an *ABAQUS* user-subroutine (**DFLUX*) in the form of an equivalent body heat flux generation. The energy-density distribution of the moving arc was assumed as a Gaussian distribution (Ref. 19) expressed by

$$q = \frac{3\eta EI}{\pi a^2}\exp\frac{(x - vt)^2 + y^2 + z^2}{-a^2/3} \qquad (5)$$

Where η is arc efficiency, v welding speed, *E* arc voltage, *I* welding current, *a* effective radius of the heat source, and t welding time. The corresponding welding parameters considered in this study are summarized in Table 1. Equation 5 was used to approximate an equivalent 3-D power density distribution of the weld region within an effective heat source radius, *a*. The final values of the effective heat source radius, *a* and arc efficiency η as shown in Table 1, were based on a series of numerical experiments to achieve a good estimation of both temperature histories at measured locations and weld zone profile, as discussed later. A similar approach has been used in a number of early studies (Refs. 18, 31) for 3-D weld residual stress predictions in aluminum alloys.

The trailing heat sink was modeled by developing an *ABAQUS* user-subroutine (**FILM*) to simulate the intense cooling effects due to the presence of a heat sink. The heat sink was assumed to follow the welding arc with a distance *D*. The resulting energy density within the heat sink area was assumed to be uniform and was expressed as

$$q_l = \frac{\eta_c Q_l V_c}{\pi b^2} \qquad (6)$$

where η_c is cooling efficiency, V_c flow

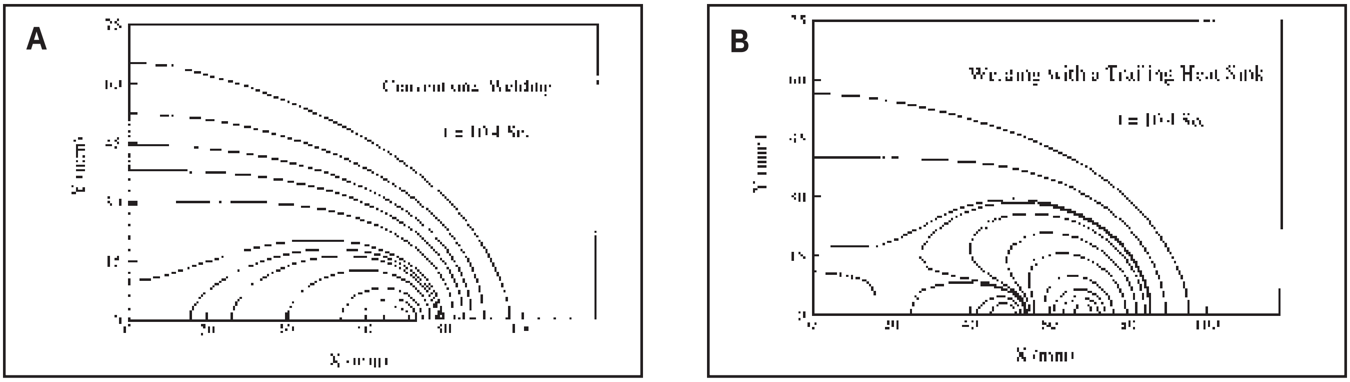

Fig. 8 — Predicted temperature distributions on top surface. A — Conventional welding; B — welding with a trailing heat sink.

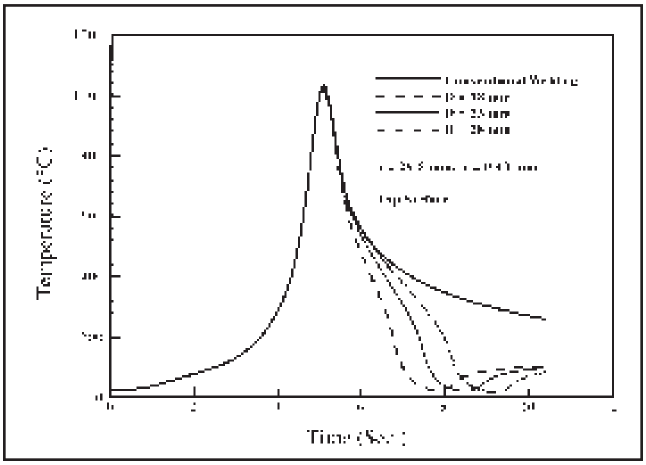

Fig. 9 — Effects of cooling distance, D, *on temperature histories.*

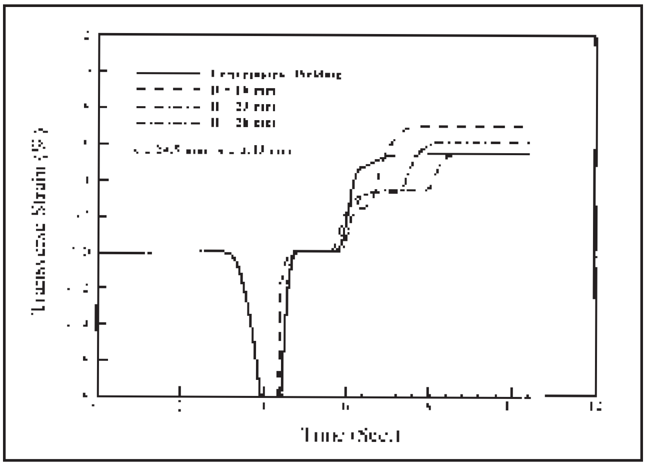

Fig. 10 — Transient strain behaviors under various cooling conditions

rate of cooling media, Q_l energy required by vaporization of cooling media and b effective radius of the heat sink area. The heat sink parameters for using liquid nitrogen are given in Table 1. The energy loss density q_l due to the presence of the trailing heat sink was considered as an equivalent convection loss effect with the following expression:

$$h_l(\theta - \theta_l) = q_l \qquad (7)$$

The equivalent convection coefficient, h_l, for the heat sink area can be calculated for a given equivalent ambient temperature θ_l. A series of numerical experiments showed the equivalent ambient temperature within the heat sink area could be assumed at –10°C to achieve satisfactory temperature predictions. The thermophysical properties for AA 2024 used in the thermal analysis are listed in Table 2 and Fig. 5 (Refs. 23, 25, 26).

Weld Constitutive Model

A unified constitutive model for welding process simulation was adopted from an early work (Ref. 27). For completeness, its relevant formulations are briefly summarized below, particularly on the definitions of some of the parameters used in this study.

By assuming additive decomposition of the strains, the rate form of the strains can be written

$$\dot{\underset{\sim}{\varepsilon}}^{Tot} = \dot{\underset{\sim}{\varepsilon}}^{e} + \dot{\underset{\sim}{\varepsilon}}^{p} + \dot{\underset{\sim}{\varepsilon}}^{\theta} + \dot{\underset{\sim}{\varepsilon}}^{A} + \dot{\underset{\sim}{\varepsilon}}^{ph} \qquad (8)$$

where $\dot{\underset{\sim}{\varepsilon}}^{Tot}, \dot{\underset{\sim}{\varepsilon}}^{e}, \dot{\underset{\sim}{\varepsilon}}^{p}, \dot{\underset{\sim}{\varepsilon}}^{\theta}, \dot{\underset{\sim}{\varepsilon}}^{A}, \dot{\underset{\sim}{\varepsilon}}^{ph}$ are the total, elastic, plastic, thermal, "annealing" and phase change strain rate tensors, respectively. The elastic, plastic, and thermal strains are defined in the classical sense. As required in welding process simulation, we postulate the existence of an "annealing strain," which is important only at near-melting temperatures. The "annealing strain" eliminates the history of prior straining above a reference temperature (such as at melting), θ_A. For instance, once reaching melting temperature, all accumulated elastic and plastic strains $\dot{\underset{\sim}{\varepsilon}}^{e} + \dot{\underset{\sim}{\varepsilon}}^{p}$ and stresses should be vanished in the context of solid mechanics analysis procedures as the material transforms from solid to liquid states. To restore such a "virgin" state , the associated annealing strain $\dot{\underset{\sim}{\varepsilon}}^{A}$ can be expressed as

$$\dot{\underset{\sim}{\varepsilon}}^{A} = -\dot{\underset{\sim}{\varepsilon}}^{A}\left(\theta, \dot{\theta}, \underset{\sim}{\varepsilon}\right) \qquad (9)$$

where $\dot{\underset{\sim}{\varepsilon}}^{A}$ is a function of temperature, its rate and strain. Neglecting solid-state phase change effects for the present discussions, the stress strain relation may be written as:

$$\dot{\underset{\sim}{\sigma}} = \underset{\approx}{E} : \left(\dot{\underset{\sim}{\varepsilon}}^{Tot} - \dot{\underset{\sim}{\varepsilon}}^{p} - \dot{\underset{\sim}{\varepsilon}}^{\theta} - \dot{\underset{\sim}{\varepsilon}}^{Ap}\right) \qquad (10)$$

where $\underset{\approx}{E}$ is the temperature dependent elastic stiffness tensor, and we distinguish between plastic $\dot{\varepsilon}^{Ap}$ and elastic $\dot{\varepsilon}^{Ap}$ annealing strains. By adopting Von Mises yield criterion within a framework of combined kinematic and isotropic hardening rule, as required in modeling

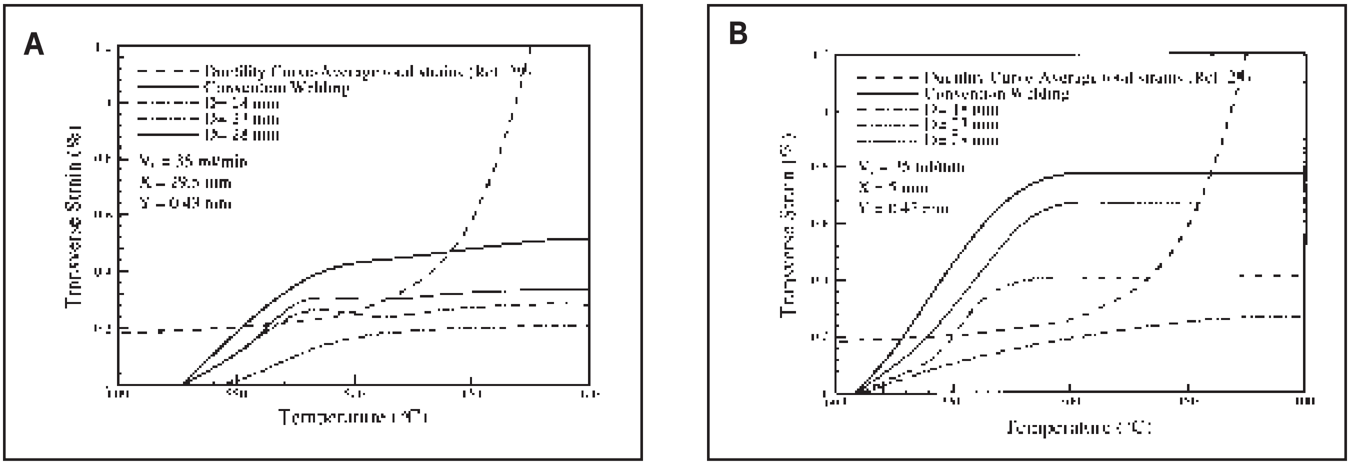

Fig. 11 — Effects of cooling distance, D, *on the development of transverse strain at two selected positions. A —* X *= 29.5 mm,* Y*= 0.43 mm; B —* X *= 5 mm,* Y *= 0.43 mm (near weld start position).*

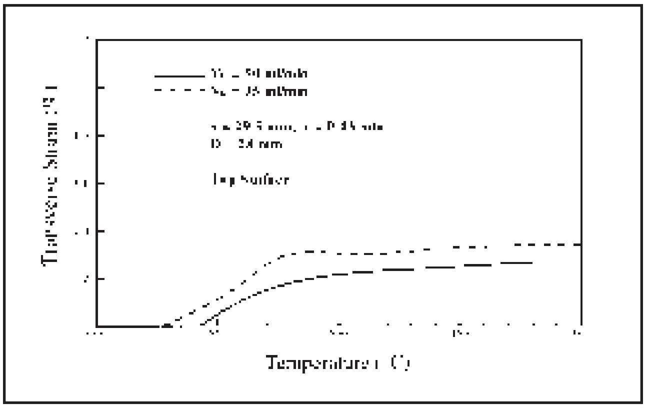

Fig. 12 — Effects of cooling intensity (cooling liquid flow rate) on transverse strain.

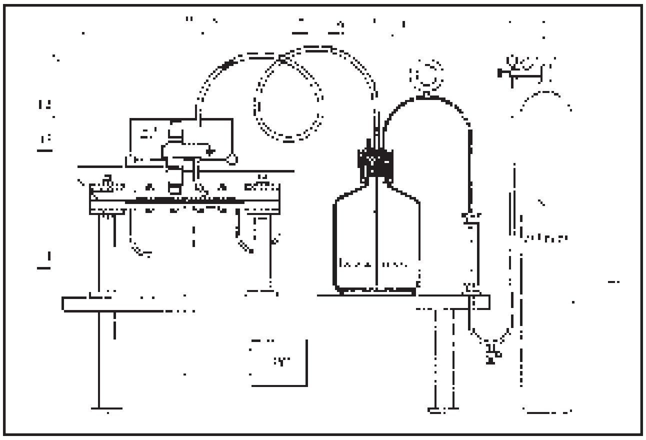

Fig. 13 — Experimental set up for GTA welding with trailing cooling.

cyclic efforts in multipass welds, the yield function can be formulated, as described in detail (Ref. 27).

For the annealing strains, we assume

$$\dot{\underset{\sim}{\varepsilon}}^{A} = 0, \qquad \text{for } \theta < \theta_A$$

$$\dot{\underset{\sim}{\varepsilon}}^{A} = \left(\frac{\dot{\theta}}{\theta_m - \theta}\right)^{m} \dot{\underset{\sim}{\varepsilon}}^{A}, \quad \text{for } \theta_A < \theta < \theta_m \qquad (11)$$

where θ_m is the material melting temperature given in Table 2, θ_A is the annealing temperature and m can be assumed to fit various material annealing behaviors. The detailed numerical implementation was discussed in Ref. 27. In the current study, it is assumed that θ_A = 450°C and $m = 1$. Other material properties used in the present analysis are shown in Fig. 6 (Refs. 24, 25). Young's modulus *E*, Poisson's ratio ν and thermal expansion coefficient α are given in Fig. 6A and yield stress σ_s and linear hardening modulus *H* in Fig. 6B.

Results and Discussions

Thermal Analysis

Under the given set of welding process parameters measured (welding current, voltage and travel speed), the final selection of arc efficiency, η and heat source radius, *a* were based on a series of numerical experiments until a good agreement with the measured temperature history and fusion profile was achieved. For instance, the predicted temperature history at the center of the specimen with x = 50 mm and y = 0 is compared with experimental results in Fig. 7 under conventional gas tungsten arc welding conditions. It can be seen a good agreement was obtained between the finite element predictions and measurements. The predicted temperature distribution on the top surface of the specimen at t = 10.4 s is shown in Fig. 8A. As a trailing heat sink was introduced behind the welding torch (Fig. 3B), a severe isotherm depression behind the weld pool can be seen in Fig. 8B. Such an isotherm depression induced by the trailing sink was intended to change the transient stress and strain behavior within the BTR region in a favorable manner. The effects of the distance, *D* between the welding torch and the trailing heat sink are shown in Fig. 9, where the temperature histories at a material point (x = 29.5 mm and y = 0.43 mm) were obtained with *D* = 18, 23 and 28 mm, respectively. It is important to note the maximum temperature reached remained the same among the three cases, but their cooling rates were altered drastically. As expected, the shortest distance (*D* = 18 mm) generated the highest cooling rate.

Thermomechanical Analysis

With the temperature histories obtained above, sequentially-coupled thermomechanical analyses were performed under conditions with and without a trailing heat sink. Predicted transverse mechanical strain (as a measure of hot cracking driving force) histories at the same material point as the one described in Fig. 9 (x = 29.5 mm and y = 0.43 mm) are shown in Fig. 10. The solid line shows the results obtained under conventional GTA welding conditions. With the approach of the welding torch, the material point was rapidly heating up and subjected to compression. After reaching its melting temperature, a zero mechanical strain state was restored at about t = 4.8 s. Note the restoration to the material's virgin state after melting would not be possible without the use of the unified constitutive law described earlier. As the welding torch was moving further away from this position, the material started solidifying, with a sudden increase in the transverse mechanical strain being predicted. It is this tensile strain increase within the BTR region that acts as the driving force for hot cracking. The effects of the distance, *D,* between the welding torch and trailing heat sink are also shown in Fig. 10. It can be seen the increase in tensile strain was significantly reduced as a trailing heat sink was introduced.

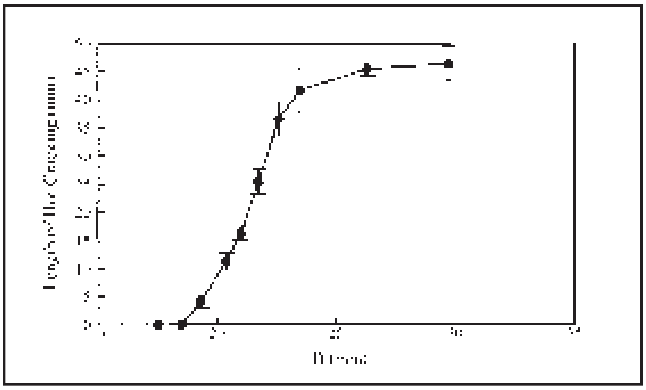

Fig. 14 — Effects of cooling distance, D*, on hot crack length — experimental results*

To illustrate the effects of the trailing heat sink on the thermomechanical conditions associated with hot cracking, the finite element results are plotted in the same format as the material's hot-ductility curve presented by Tamura (Ref. 28) in Fig. 11. As it is correctly pointed out by one of the reviewers (Ref. 29) for this manuscript, the ductility curve (solid line) was obtained by measuring averaged strains (thermal and mechanical) over a gauge length of 20-mm distance (Ref. 28). The transverse strain results from the current study are local mechanical strain values at the selected positions. With this in mind, however, some general observations can still be made by presenting the finite element results in the same format (strain vs. temperature) as the ductility data by Tamura (Ref. 28).

In Fig. 11A, the computed transverse strains as a function of temperature are shown under conditions with and without trailing heat sink conditions for the same material point (x = 29.5 mm, y = 0.43 mm) as that in Figs. 9 and 10. The

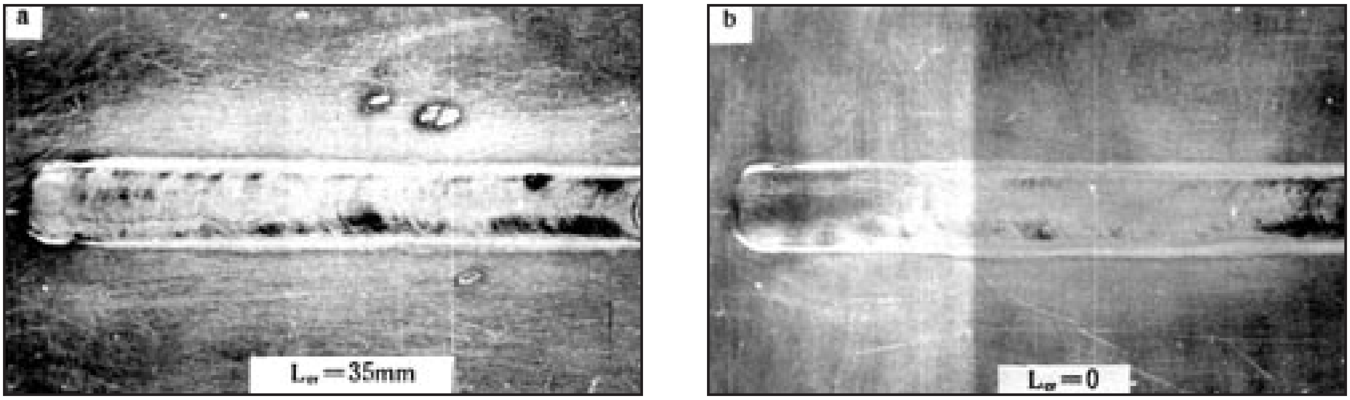

Fig. 15 — Photographs of weld samples. A — Conventional welding; B — welding with a trailing heat sink.

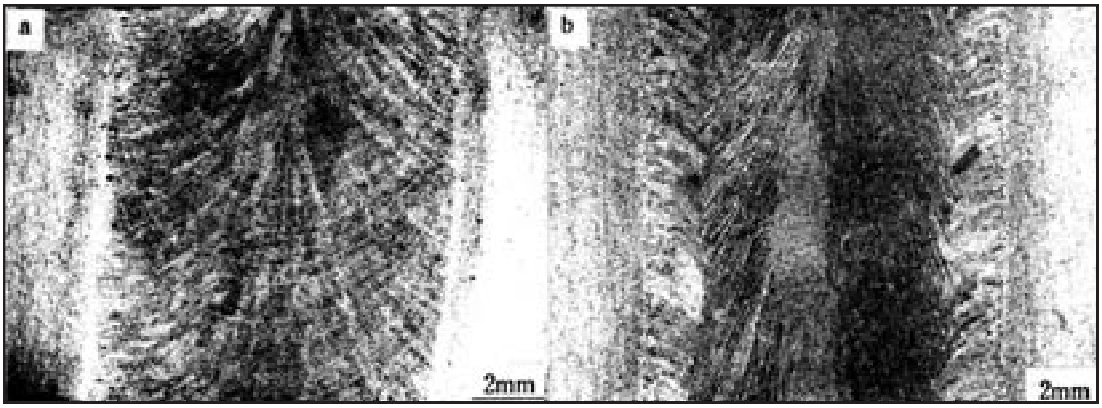

Fig. 16 — Weld crystallization orientation. A — Conventional welding; B — welding with a trailing heat sink.

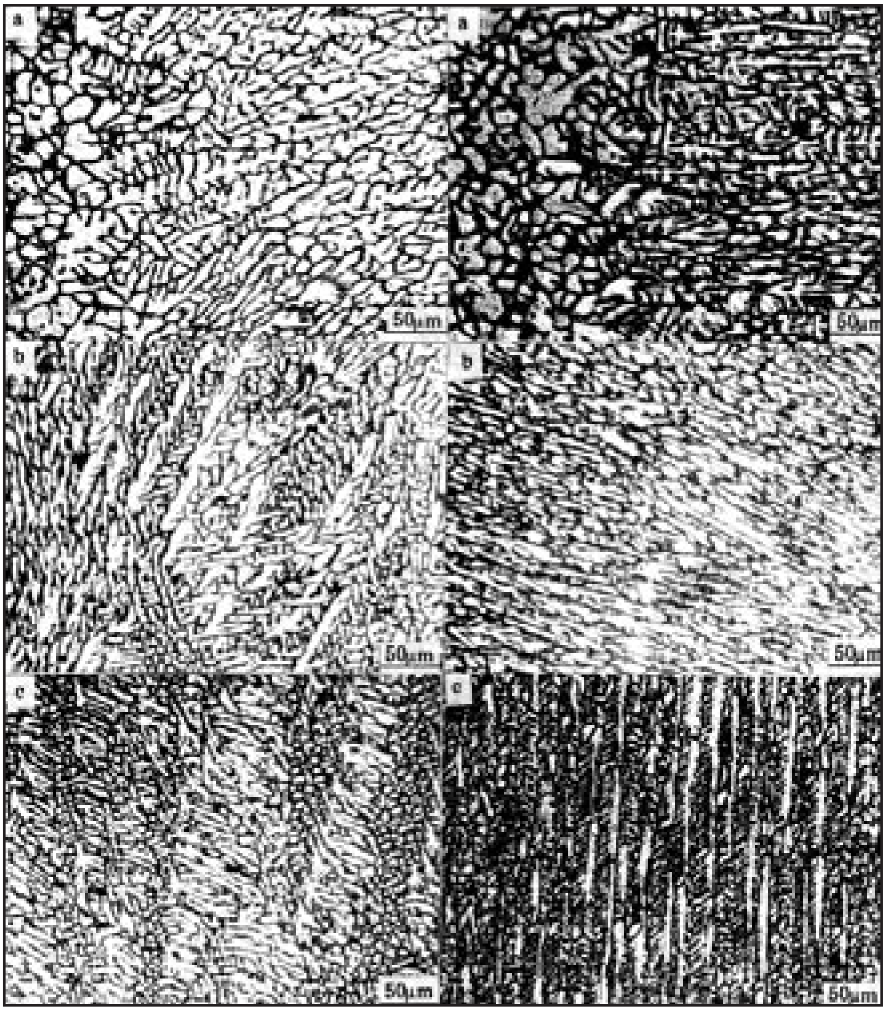

Fig. 17 — Microstructure of weld samples. A — Conventional welding; B —welding with a trailing heat sink; C — weld center.

transverse strain level under conventional GTA welding conditions (solid line) without trailing heat sink was the highest throughout the temperature range among the four cases presented. When a trailing heat sink was introduced, the transverse strain was noticeably reduced, depending on the distance, *D*, between the welding torch and the heat sink. It is known that the detailed stress/strain evolution can be a strong function of location and that hot cracking often initiates near the weld start position (Refs. 7, 8). The computed transverse strain results at a position (x = 5 mm, y = 0.43 mm) near the weld start position are summarized in Fig. 11B. The results for the four cases share a similar trend to the one shown in Fig. 11A. However, the computed transverse strain levels near the weld start position were higher than those in Fig. 11A for the position well inside the specimen, as one would expect.

Figure 12 shows the effects of the cooling intensity (cooling liquid flow rate) of the trailing heat sink on the transverse strain evolution. In this case, the distance, *D*, was kept constant at 28 mm. The results indicate that the transverse strain further decreases with an increasing cooling intensity (cooling flow rate). This is desirable since the intense cooling may be used in exchange for a longer distance between the welding torch and the heat sink so the technique can be more readily implemented in practice.

Experimental Verification

To implement the proposed welding technique with a trailing heat sink, an experimental set up was developed, as shown in Fig. 13. Liquid nitrogen was selected as a cooling media behind the welding torch. This was accomplished by using a spray nozzle connected with a pressurized liquid nitrogen supply system. The distance between the welding torch and the cooling nozzle can be adjusted for optimal performance.

As indicated in Fig. 11, the distance, *D*, between the welding torch and the trailing heat sink was identified as an important parameter in reducing the propensity for hot cracking. With the optimal process conditions being approximately established from the detailed finite element simulations discussed earlier, welding trials were performed for various values of *D*. The results are summarized in Fig. 14. It can be seen the smaller the cooling distance *D*, the shorter the hot cracking length. As the cooling distance became shorter than 18.5 mm, hot cracking was completely eliminated. Fig. 15 shows the photographs of two typical welding trial specimens with and without using the trailing heat sink method, respectively. The hot crack length under conventional GTA welding conditions was measured at 35 mm, while there was no indications of any cracks for specimens welded with the trailing heat sink (*D* = 18 mm).

Since the heat flow characteristics were significantly altered with the presence of a trailing heat sink, the corresponding weld microstructure evolution process was expected to be changed as well, such as solidification orientation, grain size, etc. As shown in Fig. 16A, grains grow from the weld interface and interlock at the weld centerline under conventional GTA welding conditions that can facilitate the forming of susceptible sites for hot cracking initiation (Ref. 30). With a trailing heat sink, as shown in Fig. 16B, grains grow from the area subjected to intensive cooling. Such a solidification pattern may have additional beneficial effects on creating favorable flow conditions for low-melting species and impurities back into the molten weld pool. A detailed investigation is underway to examine these metallurgical effects and will be reported later. In addition, the overall microstructure becomes finer than the one without the trailing heat sink — Fig. 17. These are additional metallurgical benefits resulting from the trailing heat sink.

Conclusions

The detailed mechanisms associated with weld hot cracking in aluminum alloy 2024 have been discussed in light of finite element results. A hot cracking mitigation technique was developed by introducing a trailing heat sink during GTA welding. Advanced finite element techniques were used to establish the detailed understanding of the thermomechanical process during welding. The relative importance of various cooling parameters were then derived from the finite element results. Welding trials were also conducted to verify the effectiveness of the proposed technique. The major findings are summarized as follows:

1) With the introduction of a trailing heat sink, the mechanical strain associated with hot cracking can be significantly reduced particularly within the region undergoing BTR between the weld pool and the heat sink.

2) With a proper combination of the distance *D* (between the welding torch and trailing heat sink) and cooling intensity, hot crack can then be eliminated.

3) Welding trials on aluminum alloy 2024 confirmed the effectiveness of the trailing heat sink techniques.

4) Additional benefits of microstructure refinement and more favorable grain orientation were also observed from weld samples produced by using the trailing heat sink techniques.

Acknowledgments

The authors would like to express sincere thanks to Profs. H. Zhu, M. Li and G. Zhong of Harbin Institute of Technology for their valuable suggestions and discussions during the experimental phase of this investigation.

References

1. Dvornak, M. J., Frost, R. H., and Olson, D. L. 1991. Influence of solidification kinetics on aluminum weld grain refinement. *Welding Journal* 70(10): 271-s–276-s.

2. Tseng, C., and Savage, W. F. 1971. The effect of arc oscillation. *Welding Journal* 50(11): 711–786.

3. Kou, S., and Le, Y. 1985. Alternating grain orientation and welding solidification cracking. *Metallurgical Transactions* 16A(10): 1887–1896.

4. Kou, S., and Le, Y. 1985. Improving weld quality by low frequency arc oscillation. *Welding Journal* 64(3): 51–55.

5. Matsuda, F., Nakata, K., and Uchiyama, T. 1984. Effect of addition element on weld solidification cracking susceptibility of Al-Zn-Mg alloy (Report III). *Transactions of JWRI* 13(1): 57–66.

6. David, S. A., and Vitek, J. M. 1989. Correlation between solidification parameters and weld microstructures. *International Materials Review* 34 (5): 213–245.

7. Zacharia, T. 1994. Dynamic stresses in weld metal hot cracking. *Welding Journal* 73(7): 164-s–172-s.

8. Feng, Z. 1994. A computational analysis of thermal and mechanical condition for weld metal solidification cracking. *Welding in the World* 33(5): 340–347.

9. Karlsson, L. 1976. Stress Fields Induced by Moving Heat Source in Butt-Welding of Plates. Ph.D. dissertation. Chalmers University of Technology, Goteborg, Sweden.

10. Sekiguchi, H., and Miyake, H. 1975. Prevention of welding cracks through a local heating process. *Transactions of the Japan Welding Society* 6(1): 59–64.

11. Sekiguchi, H., and Miyake, H. 1975. Postheating of the welding part of steel through a local heating process. *Transactions of the Japan Welding Society* 6(1): 53–58.

12. Hernandez, L. E., and North, T. H. 1984. The influence of external local heating in preventing cracking during welding of aluminum alloy sheet. *Welding Journal* 63(3): 84-s–90-s.

13. Hernandez, I. G. 1977. Nature and Prevention of Solidification Cracking in Welds. Ph.D. dissertation. Strathclyde University, Glasgow, Scotland.

14. Wu, E. 1990. A Study of Solidification Cracking of Cr-Ni Austenitic Stainless Steel. Ph.D. dissertation. Tsing Hua University, Beijing, China.

15. Liu, W., Tian, X., and Zhang, X. 1996. Preventing weld hot cracking by synchronous rolling during welding. *Welding Journal* 75(9): 297-s–304-s.

16. *ABAQUS/Standard User's Manual.* 1995. Hibbitt, Karlsson & Sorensen, Inc., Version 5.5.

17. Zhang, J., Dong, P., Brust, F. W. 1997. Composite shell element model for residual stress analysis of multi-pass welds. *Transaction of the 14th International Conference on Structural Mechanics in Reactor Technology*, ed. Michel Livolant, (1): 335–344. The International Association for Structural Mechanics in Reactor Technology.

18. Dong, P., Hong, J. K., and Rogers, P. 1998. Analysis of residual stresses in Al-Li alloy repair welds and mitigation techniques. *Welding Journal* 77(11): 439-s–445-s.

19. Kou, S. 1987. *Welding Metallurgy.* pp. 393–395. John Wiley & Sons.

20. Rose-Innes, A. G. 1965. *Low Temperature Technique,* p. 140. D. Van Nostrand Company, Inc.

21. Necati, O. M. 1993. *Heat Conduction.* p. 14. John Wiley & Sons, Inc.

22. Sparrow, E. M. 1978. *Radiation Heat Transfer,* p. 45. Mcgraw Hill Book Company.

23. Pehlke, R. D., Jeyarajan, A., and Wada, H. 1982. Summary of thermal properties for casting alloys and mold materials, pp. 82–93. National Technical Information Service.

24. ASM Handbook Committee. 1979. *Metals Handbook* Ninth Edition, Vol. 2, Properties and selection: nonferrous alloys and pure metals, p. 68, 72–74. ASM International, Materials Park, Ohio.

25. Davis, J. R. 1994. *ASM Specialty Handbook*, pp. 653–654. The Materials Information Society.

26. Victor, J. J. 1990. *A Compendium of the Properties of Materials at Low Temperature* (Phase I), pp. 2.132, 3.132, 4.132. Wright Air Development Division.

27. Brust, F. W., Dong, P., Zhang, J. 1997. A constitutive model for welding process simulation using finite element methods. *Advances in Computational Engineering Science*, ed. by S. N. Atluri and G. Yagawa, pp. 51–56. Tech Science Press.

28. Tamura, H. 1977. Cracking study of aluminum alloys by the variable tensile strain hot cracking test. *Transaction of the Japan Welding Society* 8(2): 63–69.

29. Principal Reviewer's Comments, Nov. 1998.

30. ASM International Handbook Committee. 1997. *ASM Handbook*, Vol. 6, Welding, brazing, and soldering, p. 88. ASM International, Materials Park, Ohio.

31. Dong, P., Hong, J. K., Zhang, J., Rogers, P., Bynum, J., and Shah, S. 1998. Effects of repair weld residual stresses on wide-panel specimens loaded in tension. *ASME Journal of Pressure Vessel Technology* 120(2): 122–128.

Call for Papers

EPRI is sponsoring the Aging Workforce and Educational Infrastructure Conference and Exhibition, June 12–15, 2000, in Charlotte, N.C. The conference will address the methods and needs of maintaining capabilities of an aging workforce and declining education infrastructure. Some areas of interest are computer-based training, distance learning, proficiency testing, cross training, simulators and application of the Internet for education. Individuals or organizations interested in making a presentation should submit a 1–2-page abstract to Ken Brittain, conference manager, at *kbrittai@epri.com*. Abstracts are due March 1, 2000.